MODELLING OF ELECTRODE-ARC COUPLING IN ELECTRIC ARC WELDING

Alireza Javidi Shirvan[1], **Isabelle Choquet**[1], **Håkan Nilsson**[2]

[1] *University West, Dept. of Engineering Science, Trollhättan, Sweden,*
[2] *Chalmers University of Technology, Dept. of Applied Mechanics, Gothenburg, Sweden*

alireza.javidi@hv.se

Abstract: Modelling of the arc in electric arc welding is significant to achieve a better process understanding, thus gain better weld quality and a more efficient production process. It requires knowing the conditions at the surfaces of the anode and cathode. These conditions are very difficult to set from measurements and should be calculated. This requires modelling the complex physics of the electrode layer coupling electrode and arc. This paper presents a self-consistent electrode layer model that 1) is suited to welding applications, 2) accounts for the known physics taking place, and 3) satisfies the basic conservation requirements. The model is tested for different conditions. Its potentiality for welding applications is shown through calculations coupling plasma arc, electrode and cathode layer models. The calculations are done for both tungsten and thoriated tungsten electrode.

Keywords: thermal plasma, arc welding, electrode layer, sheath, electrode surface temperature, numerical simulation, OpenFOAM.

1. INTRODUCTION

An important issue in welding manufacturing is to avoid the formation of defects during production. Some of the most common weld defects are lack of fusion, porosity, solidification cracks and spatters. They weaken the welded component thus increasing the risk of failure. When detected during production additional repairing processing can be needed. To minimize welding defects and make the process more resource efficient and sustainable many research studies have been done, most of them being experimental. Nevertheless, due to the extreme conditions met in welding (very high temperature gradients in a very narrow region) experiments do not yet allow measuring all the quantities of interest for better understanding and controlling the process. Modelling and simulation provide a complementary source of information.

Today modelling mainly covers the behavior of the weld pool, changes in material microstructures and properties and residual stresses of the weld. This require input data such as the heat input into the base metal due to the electric arc. In most cases this heat input is specified imposing a semi-empirical heat source profile into the base metal. This approach involves parameters that are adjusted to reproduce as closely as possible experimental weld geometries. An advantage is the simplicity of the approach but the main drawback is the need for experimental data for setting the unknown parameters for each case. An alternative would be to employ input data delivered by a welding arc simulation model. Arc simulation provides also additional information. For instance it allows doing the distinction between the different sources of heat transfer (due to conduction and charge diffusion for instance), and investigating how they are influenced by the different process parameters.

The first thermal plasma simulation model was introduced in 1983 by Hsu *et al.* (1983). This model was developed for long and axisymmetric arcs (so-called transferred arc) assuming a negligible radial current density. It is now know that this assumptions is not suited to the shorter arcs met in welding, see (Choquet *et. al*, 2012). From late 1990's many studies have been started to extend the modelling of thermal plasma arc to the particular welding setting. A review can be found in the thesis by Sass-Tisovskaya (2009).

The physical phenomena taking place in an electric arc discharge are not uniform. For this reason sub-regions are distinguished, as sketched in Figure 1. The main sub-regions are a) the plasma core, b) the anode and cathode, and c) the anode and cathode layers.

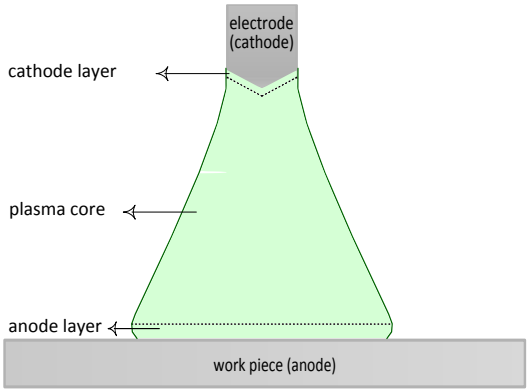

Fig. 1. Sketch of the sub-regions of an arc discharge (GTAW).

• The plasma core represents the main body of the plasma. Its characteristic size is large compared to the Debye length and the mean free paths. It implies that the plasma core is globally quasi neutral and the continuum approach is valid as partial local thermodynamic equilibrium (LTE) is satisfied (Choquet and Lucquin-Desreux, 2005). In the regions with low collisional frequency between the light particles at temperature T_e (i.e. the electrons) and the heavy particles (i.e. atoms and ions) at temperature T_h, LTE is only partial so that $T_e \neq T_h$. These regions use to be confined to the cold plasma edges while the body of the plasma core is at thermal equilibrium ($T_e = T_h$). The recent comparative study done by Freton *et al.* (2012) shows that the various models developed up to now to account for partial LTE at the colder plasma edges still present inconsistencies since they are based on Saha laws that do not satisfy entropy inequality (Choquet and Lucquin, 2005). For all these reasons the plasma core is modelled here assuming LTE. This model couples thermal fluid mechanics (governing plasma mass, momentum, and energy or enthalpy) with electromagnetics (governing the magnetic field, the electric field and the current density) for a temperature range from 200K up to 30000K, see (Choquet *et al.* 2012).

• The anode and cathode (also called work piece and electrode in welding) are in solid state and can be partially liquid. In Gas Tungsten Arc Welding (GTAW) the refractory tungsten electrode is usually the cathode and the work piece is the anode. In Gas Metal Arc Welding (GMAW) it is usually the opposite. In academic studies of GTAW the work piece is often water cooled so that electrode and work piece are maintained in a solid state. In industrial applications the work piece is partially melted (weld pool) and the electrode may also be diphasic (in GMAW). It should be noted that melting is not addressed in this study. The model used for this region thus couples a thermal energy conservation equation with electromagnetics (governing the magnetic field, the electric field and the current density), see (Javidi, 2013).

• The cathode layer (resp. anode layer) is the interface allowing the coupling between cathode (resp. anode) and plasma core. The cathode layer is critical since the plasma formation and conversion from electric to thermal energy take place in this layer. The primary focus of this study is thus on the cathode side. As shown by Füssel *et al.* (2014), the level of accuracy of the cathode model has a significant impact on quantities of importance for welding applications, namely the heat fluxes to the work piece and the arc pressure force on the work piece.

Today, most of the electric arc simulation studies done to investigate welding applications are still restricted to the plasma core and omit the solid regions and their layers, see (Sass-Tisovskaya, 2009). To calculate a plasma core model boundary conditions need to be set on the cathode and anode surfaces. These boundary conditions are derived from experimental data which are very difficult to measure in the region of interest, thus their lack of accuracy. Moreover, very few documented cases are available.
To avoid these drawbacks, the plasma core simulation model has been extended by Sansonnens *et al.* (2000) and then by Lowke and Tanaka (2006) to include a solid cathode region (GTAW) and simplified cathode layer models (further details are given in section 3). Their simplifications imply that these models do not satisfy current density conservation. A recent comparative study done by Füssel *et al.* (2014) shows that the most accurate of these two models (Sansonnens *et al.* 2000) underestimates the heat flux to the work-piece while it overestimates the pressure force applied by the arc on the work piece. These cathode layer models may thus be too simplified.
In parallel, and independently of any welding application, physicists investigate in detail the physics taking place within the cathode layer. This started long ago with the first studies published by Tonks and Langmuir, as well as

Mackeown in 1929. Today, this topic is still actively investigated. A rather recent review was done by Benilov (2008) and more recent bibliographic studies can be found in (Cayla, 2008) and (Javidi, 2013). The first coupling between the comprehensive cathode layer model developed in physics and a plasma core model was done by Cayla and applied to a so-called transferred arc assuming a flat electrode (Cayla, 2008). This coupling has not yet been established within the frame of welding applications.

The aim of this work is to develop a self-consistent arc-electrode model that 1) is suited to welding applications, 2) accounts for the relevant physics, and 3) satisfies the basic conservation requirements (e.g. current and energy). The physics taking place in the cathode layer is described in section 2. The cathode layer model is presented in section 3. It is based on Benilov's model (Benilov and Marotta, 1995), (Benilov, 2008). It accounts also for the improvements achieved by Cayla (2008). And it was completed to fully satisfy the basic conservation principles (Javidi, 2013). For validation purposes this model is first applied to the cathode layer alone and the results are discussed in section 5. To show its potentiality for welding applications, simulations results calculated coupling the plasma core, the cathode and the cathode layer model are also presented and discussed in section 5 considering both a tungsten electrode and a thoriated tungsten electrode. Section 6 contains concluding remarks and perspectives.

2. CATHODE LAYER - PHYSICS

The cathode layer uses to be divided into two main sub-regions based on distinct leading physical phenomenon (Benilov, 2008): the sheath and the pre-sheath, see figure 2-a.

• The cathode sheath is adjacent to the cathode. It is mainly made of positive ions attracted by the negative charge of the cathode surface. The sheath, also called the space charge layer, is thus a positive layer inducing a sheath potential U_s. This layer is almost collisionless since its thickness is less than a mean free path (Cayla, 2008). It is thus modeled at the kinetic scale since the continuum approach does not apply. It has three main roles. The first one is to enhance electron emission from the cathode by lowering the surface potential barrier thanks to the sheath potential U_s. The second role is to accelerate the electrons emitted by the cathode surface as they cross the sheath towards the next layer (or pre-sheath). As a result part of the emitted electrons can reach a kinetic energy large enough to ionize atoms (and possibly ions) present in the pre-sheath. The third role is to accelerate the ions generated in the pre-sheath towards the cathode surface. Ions reaching the cathode surface with an energy lower than the surface potential barrier (or energy threshold to extract a cathode electron) do contribute to the so-called field enhanced thermoionic emission (for refractory metals) or to the field enhanced emission (for non-refractory metals), (Vacquié, 2000). The others promote the emission of the so-called secondary electrons (Cayla, 2008).

• The cathode pre-sheath, also called the ionization layer, is located between the sheath and the plasma core. In this region charged species are produced, leading to plasma formation. The ionization reaction are not at equilibrium: they are not balanced by charge recombination (Vacquié, 2000). In this layer the kinetic energy gained by the electrons in the electric field is also transferred in the form of thermal energy to atoms and ions during collisions. The thickness of this layer is much larger than the Debye length, implying global charge neutrality. The continuum

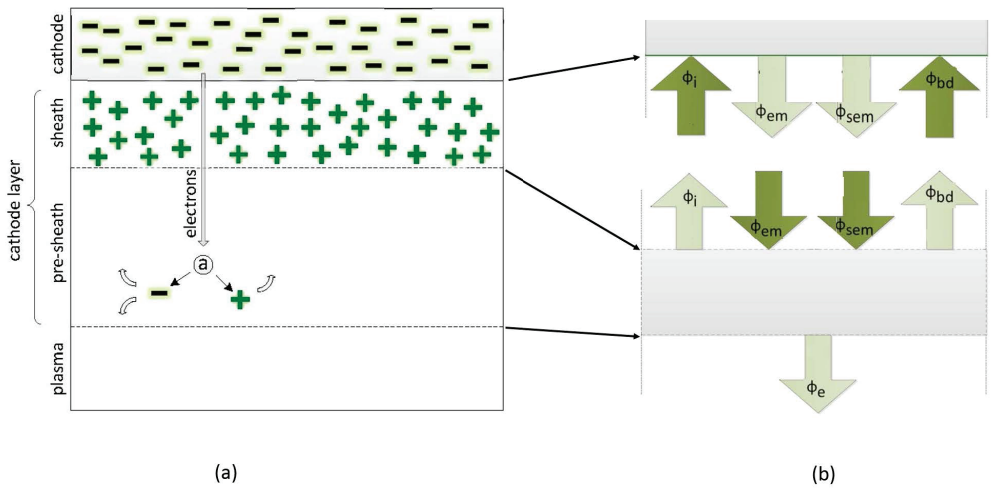

Fig. 2. Schematic sketch of: (a) a cathode layer and (b) the charge fluxes at the interfaces.

approach can be used since the pre-sheath thickness is larger than the mean three paths. However local thermal equilibrium (LTE) is only partial (Choquet *et al.* 2011). It means that the light electrons do not reach the same temperature as the heavy atoms and ions (with Te > Th). The different deviations from equilibrium in the different regions and the resultant modelling approaches are summarized in table 1.
Due to the physics taking place in both the sheath and the pre-sheath, the heat transferred from the plasma core towards the cathode is not the heat received by the cathode surface. Similarly, the charge flux emitted by the cathode surface is not the charge flux entering the plasma core. The aim of the cathode layer model is thus to provide the relations allowing coupling energy and current density between the plasma core model and the cathode model.

Table 1. Thermal, ionization and charge conditions in the different regions and resultant modelling approach.

Region	Thermal equilibrium	Ionization equilibrium	Charge equilbrium	Modelling approach
Sheath	not defined	no ionization	no neutrality	kinetic
Pre-sheath	only partial : $T_e \neq T_h$	net production of ions	global neutrality	continuum at partiel LTE
Plasma core	equlibrium: $T_e \simeq T_h$	at equilibrium	global neutrality	continuum at LTE

3. CATHODE LAYER - MODEL

The cathode layer model is based on Benilov's model (Benilov and Marotta, 1995), (Benilov, 2008). It accounts also for the improvements achieved by Cayla including the contribution of the secondary emission (Cayla, 2008). And it was completed to fully satisfy the basic principle of energy conservation at the sheath/pre-sheath interface (Javidi, 2013). The main elements of this model are summarized below. A more detailed presentation can be found in (Javidi, 2013).

The model is based on the basic principles of charge and energy conservation. The first step consist in tracking the fluxes of charged particles and the related energy fluxes through the cathode/sheath interface and through the pre-sheath. In the collisionless sheath it is assumed that the electron temperature remains equal to the electron temperature at the sheath/pre-sheath interface T_e (Benilov and Marotta, 1995) while the ion temperature T_h remains equal to the cathode surface temperature T_c (Zhou and Heberlein, 1999).

Charge conservation at the cathode/sheath interface implies that the current density J_{cath} at the cathode side is equal to the net charge flux at the sheath side. This net charge flux is made of four contributions, see Figure 2 b). Two concern the electrons emitted at the cathode surface and flowing towards the sheath. For the operating conditions met in GTAW the electron fluxes are due to the field enhanced thermoionic emission ϕ_{em} and the secondary emission ϕ_{sem}. The two remaining contributions are due to the charged particles flowing in the opposite direction (from the sheath towards the cathode) as a result of impact ionization in the pre-sheath, see Figure 2 a). They include the positive ion flux ϕ_i and the back diffusion electron flux ϕ_{bd}. The conservation of the current density at the cathode/sheath interface thus writes

$$J_{cath} = e\left[\phi_{em}(T_c,U_s) + \phi_{sem}(n_i,T_c,T_e,U_s) + Z\phi_i(n_i,T_c,T_e,U_s) - \phi_{bd}(n_e,T_e,U_s)\right] \tag{1}$$

where e denotes the electron charge and Z the average ion charge number. The current at the cathode surface J_{cath} is the input parameter of the cathode layer model; it is provided by the cathode model (see section 1). ϕ_{em} is given by Richardsson emission formula supplemented with Schottky correction (Javidi, 2013). It depends on T_c and U_s. ϕ_{sem} is given by Lichtenberg expression (Javidi, 2013) and is proportional to ϕ_i. ϕ_i depends on the ion densities n_i at the sheath/pre-sheath interface, T_c and T_e (via Bohn velocity), and the accelerating sheath potential U_s (Javidi, 2013). Finally ϕ_{bd} depends on the electron density n_e at the sheath/pre-sheath interface, T_e and U_s (Javidi, 2013). Equation (1) thus depends on the five variables n_i, n_e, T_c, T_e and U_s.

Energy conservation at the cathode/sheath interface implies that the energy flux q_{cath} at the cathode side is equal to the net energy flux at the sheath side. The heat flux q_{cath} is then dissipated in the cathode bulk by thermal conduction. The energy at the sheath side is transported by the same charge fluxes as the current densities in Equation (1). The energy conservation at the cathode/sheath interface writes

$$\begin{aligned} q_{cath} = &-\left(\varphi_{eff} + 2kT_c\right)\left[\phi_{em}(T_c,U_s) + \phi_{sem}(n_i,T_c,T_e,U_s)\right] \\ &+ (0.5kZT_e + ZeU_s + E_{ion} - Z\varphi_{eff})\phi_i(n_i,T_c,T_e,U_s) + \left(\varphi_{eff} + 2kT_e\right)\phi_{bd}(n_e,T_e,U_s) \end{aligned} \tag{2}$$

wheree k is Boltzmann constant, E_{ion} the ionization energy and φ_{eff} the effective work function of the cathode

material. The terms weighting the different particle fluxes ϕ do represent the amount of energy transported by each charge flux. The cathode electrons with an energy larger than φ_{eff} are emitted towards the sheath (half space) with a kinetic energy at thermal equilibrium with the cathode surface at T_c. The energy transferred to the cathode by ions with a velocity large enough to pass the sheath include a kinetic contribution (two first terms) and a source (two last terms) due to ion recombination at the cathode surface. Finally the back diffusion electrons reaching the surface are only those with a kinetic energy large enough to pass the adverse sheath potential. The derivations allowing obtaining Equation (2) are further detailed in (Javidi, 2013).

Energy conservation in the pre-sheath implies that the net energy transferred from the pre-sheath at the boundary with both the sheath and the plasma core is equal to the pre-sheath energy source. This source is the net work W_E done by the electric field on all the charged particles flowing through the pre-sheath. The particle fluxes at the pre-sheath boundary can be seen in Figure 2 b). They respectively transport the energy fluxes q_{em}, q_{sem}, q_i and q_{bd}. The energy fluxes at the interface pre-sheath/plasma core include the thermal energy of the heavy particles conducted from the plasma q_{plasma} and the enthalpy and diffusion energy carried by the electrons towards the plasma q_e. The energy balance in the pre-sheath writes

$$q_{em} + q_{sem} - q_i - q_{bd} + q_{plasma} - q_e = W_E \tag{3}$$

When further developed as function of the five variables (n_i, n_e, T_c, T_e and U_s) and re-arranged, see (Javidi, 2013), it reads

$$\begin{aligned} &\left[2kT_c + eU_s + kT_e\left(\ln\frac{n_{e\infty}}{n_e} - 3.2\right)\right]\left[\phi_{em}(T_c,U_s) + \phi_{sem}(n_i,T_c,T_e,U_s)\right] = \\ &\left[2kT_i + E_{ion} + ZkT_e\left(3.7 - 0.5\ln\frac{n_{e\infty}}{n_e}\right)\right]\phi_i(n_i,T_c,T_e,U_s) + \left[eU_s + kT_e\left(\ln\frac{n_{e\infty}}{n_e} - 1.2\right)\right]\phi_{bd}(n_e,T_e,U_s) \end{aligned} \tag{4}$$

where $n_{e\infty}$ is the electron number density at the interface with the plasma core (it is thus defined at thermal equilibrium).

This system of three equations (1), (2), and (4) is supplemented with closure relations for calculating the particle densities n_i and n_e at the sheath/pre-sheath interface as well as $n_{e\infty}$ at the plasma interface. The closure equations include a set of Saha equations with Van de Sanden formulation function of T_e, supplemented with the Dalton equation for the pressure and the charge neutrality equation (Javidi, 2013).
For an argon shielding gas for instance the ions present in a welding application are Ar^+, Ar^{2+} and Ar^{3+} implying three Saha equations for closing the cathode layer model. The cathode layer model is then a system of eight nonlinearly and coupled equations. It is calculated with an iterative procedure (Javidi, 2013). A loop consist in solving the system of closure equations setting U_s, T_c and T_e, then calculating the different charge fluxes ϕ, and next solving the system of conservation equations (1), (2), (4) to update U_s, T_c and T_e. Convergence is reached in about 5 iterations of the loop.

This model depends on the cathode material through the value of the work function φ_{eff}. It depends on the type of material (refractory or not) through the expression of the electron emission flux ϕ_{em}. And it depends on the gas through the set of Saha equations. When the cathode melts as in GMAW, the energy equation (2) needs to be supplemented to account for vaporization, and the Saha equations to account for metal vapor. Finally, it should be noticed that as anode and cathode layers obey a similar concept this model can also be applied to the anode layer (Benilov, 2008).

4. RESULTS

All the applications are performed using an argon gas at atmospheric pressure. Two types of refractory cathodes are considered: tungsten and thoriated tungsten with a work function of 4.55 and 3 eV, respectively. Two sets of calculations are presented. The first set concerns the cathode layer model alone. To our knowledge the only published data of measurements done on the cathode surface are at low pressure (0.26 MPa) for a model lamp (Luhmann *et al.* 2002). The cathode layer model was compared to these data and very good agreement was obtained in (Cayla, 2008). However the standard pressure of welding applications is 1 atm. The results obtained here are thus compared with the calculation results of Cayla (2008) at 1 atm for tungsten and a cathode current density J_{cath} ranging from 1×10^4 to $5\times10^8 A.m^{-2}$. This is also the range covered in standard GTAW. For simplicity the calculations were first done using MATLAB. The cathode layer model was then implemented and tested in the CFD software OpenFOAM (where the plasma core model is already implemented (Choquet *et al.* 2012)). As expected, both software do provide the same results. Figure 3-a) illustrates the current densities in the sheath plotted versus the cathode current density J_{cath} for a tungsten cathode. It can be seen that the ion current density

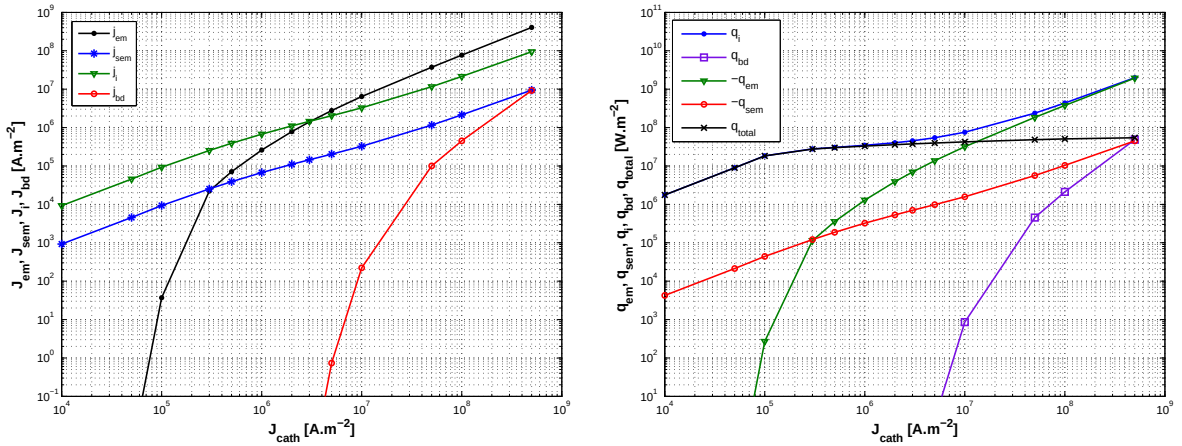

(a) (b)

Fig. 3. (a) Current densities and (b) heat fluxes against the cathode current density for a tungsten electrode.

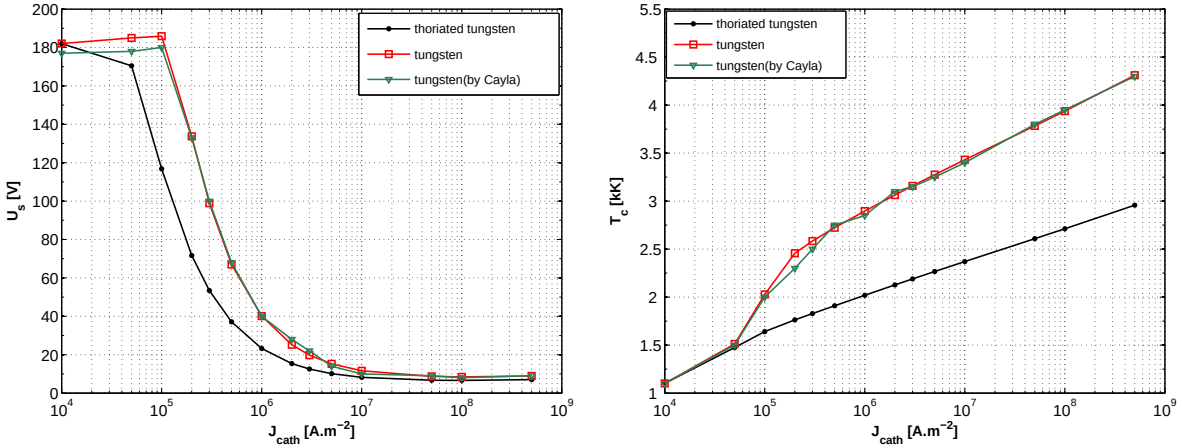

(a) (b)

Fig. 4. (a) Sheath voltage and (b) cathode temperature against the current density.

J_i is dominant when $J_{cath} \leq 2 \times 10^6 A.m^{-2}$. At larger values of J_{cath} the dominant current density is instead the field enhanced thermoionic emission J_{em}. It should be noticed that the simplified cathode layer model developed by Lowke and Tanaka (2006) for welding applications neglects J_{em}. It can be observed that the secondary emission J_{sem} is the dominant emission process ($J_{sem} > J_{em}$) when the cathode current density is less than $5 \times 10^5 A.m^{-2}$. However secondary emission is not taken into account by the simplified cathode layer models (Sansonnes *et al.* 2000) and (Lowke and Tanaka, 2006) used for welding applications. Figure 3-b) shows the total heat flux to the cathode ($q_{total} = q_{cath}$) and its components versus the cathode current density J_{cath} for a tungsten cathode. It can be seen that up to $2 \times 10^6 A.m^{-2}$ of current density, the total heat flux to the cathode is almost equal to the ion heat flux q_i. For larger cathode current density q_{total} becomes lower than q_i and it remains constant at about $2 \times 10^7 W.m^{-2}$. This is due to the high cooling effect of the emitted electrons. This cooling is not taken into account in (Lowke and Tanaka, 2006). Figure 4-a) shows the sheath voltage U_s versus the cathode current density J_{cath}. It can be seen that U_s is almost constant and at a minimum value of the order of 10 eV when $J_{cath} \geq 10^7 W.m^{-2}$. In this range the cathode surface temperature T_c is large enough to promote termoionic emission. When going down towards lower values of J_{cath}, the sheath potential U_s increases to compensate with field enhanced emission the lower thermoionic emission. It should be noticed that the electric potential in the plasma core of a welding arc is of same order as the minimum value obtained for U_s. However the simplified cathode layer models (Sansonnes *et al.* 2000) and (Lowke and Tanaka, 2006) do neglect U_s. Figure 4-b) shows the cathode surface temperature T_c versus the cathode current density J_{cath}. For tungsten and J_{cath} between 10^4 and $10^6 A.m^{-2}$, where the transition from dominant seconday emission to field-enhanced thermoionic emission and then thermoionic emission successively take place, T_c increases significantly and non-linearly. At larger values of J_{cath} thermoionic emission is established, the cathode heat flux q_{total} is constant, and T_c increases linearly. It is worth reminding that melting is not considered in this

study which makes possible for the cathode surface to reach $5300K$ while the tungsten melting point is $3682K$. Figure 4 a) and b) show also a good agreement with the data obtained by Cayla. Finaly thoriated tungsten leads to a significantly lower cathode surface temperature, as well as a lower sheath potential, compared to pure tungsten. This is an expected consequence of its lower work function.

The second set of calculations concerns the cathode sheath model coupled with the cathode bulk and the plasma core models in OpenFOAM. The cathode is cylindrical with a radius of 10 mm and the arc has a length of 5 mm. This case differs from GTAW applications due to the large cathode radius. It was chosen for testing further the model by comparison with (Cayla, 2008). The geometry and computational domain are represented in Figure 5. The cathode sheath layer model is applied at the interface GH while BH is a non-conducting surface. A temperature of 1000K is imposed on AB (water cooled cathode) as well as a uniform current of 200A. AGF is a symmetry axis. BCD is a non-conducting boundary. On the anode surface (DEF) the electric potential is set to zero. The plasma core region (BCDFGH) is initially filled with argon gas a 1 atmosphere. The boundary BCD is open to free flow at 1000K in case of inflow and no temperature gradient in case of outflow. The anode surface ED is set to 1000K while a no gradient condition is imposed on EF. The calculations were done for both tungsten and thoriated tungsten cathode. Iso-contours of current density and temperature in the plasma core are plotted in Figures 6-a) and 6-b) respectively for a tungsten electrode. Thanks to the cathode layer model these results could be obtained without imposing any temperature and current density profile on the cathode surface. This is an important advantage of this model: it needs only standard input process parameters and is independent of case specific measurements in the hot regions. The temperature plot along the vertical line with 1 mm offset from the symmetry axis is shown in Figure 6-c). It can be seen that the lower temperature obtained on the thoriated tungsten surface compared to a tungsten cathode (see Figure 4-b)) results also in a lower plasma temperature.

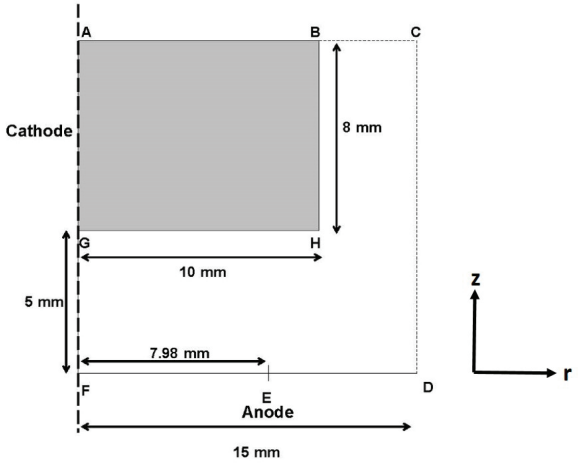

Fig. 5. Geometry and computational domain with cathode (ABHG) and plasma core (BCDFGH), (Cayla, 2008).

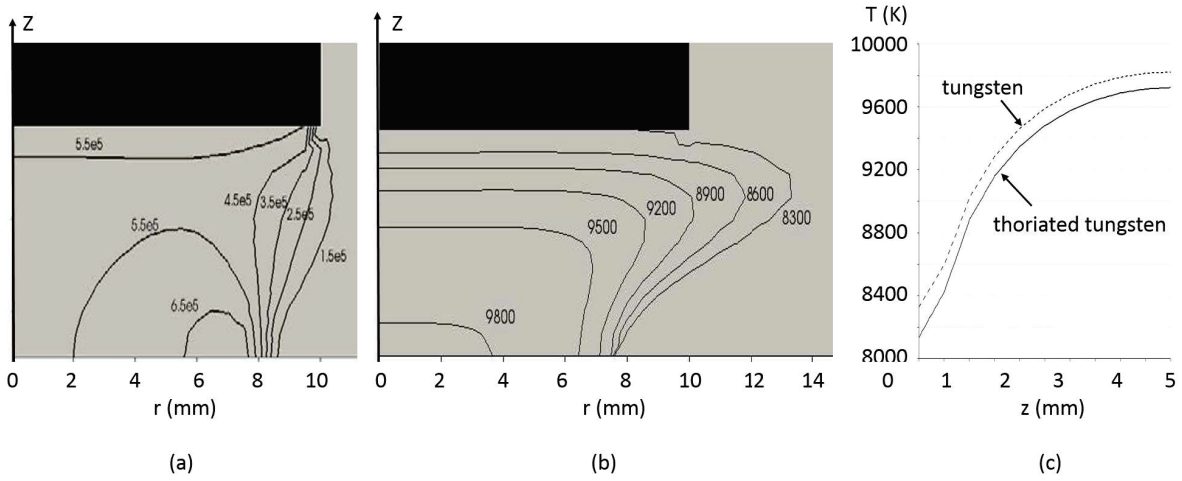

(a) Current density (A.m^{-2}) and (b) temperature (K) in the plasma core for a tungsten cathode;
(c) plasma core temperature along z in r = 1 mm.

CONCLUSION

The aim of the present work was to go one step further in the development of a predictive arc simulation model. A predictive tool would indeed allow reaching a deeper process understanding and thereby improving the process. To be predictive, the arc model should be free of boundary conditions imposed on the cathode surface.
A self-consistent cathode layer model that 1) is suited to welding applications, 2) accounts for the known physics taking place, and 3) satisfies the basic conservation requirements has been implemented and tested. It was shown that the calculation results are in good agreement with the available reference literature (Cayla, 2008). Preliminary results obtained coupling cathode, cathode sheath and plasma core show the model potentiality. They also show that the temperature and current distributions provided by the cathode sheath model have an impact on the plasma core (e.g. on its temperature distribution). The cathode layer model was discussed and important differences compared to the simplified cathode layer models used in welding applications were underlined. Some of the simplifications done, for instance neglecting the cathode sheath voltage, could explain the discrepancies observed by Füssel *et al.* (2014).
Direct confrontation to experimental data measured on the cathode surface within the frame of welding is problematic since such data do not seem to be published yet. Indirect comparison can however be done using measurements of the heat fluxes to the base metal. This will be the aim of the next step of this work.

ACKNOWLEDGMENT

This work was supported by KK-foundation in collaboration with ESAB. Håkan Nilsson was in this work financed by the Sustainable Production Initiative and the Production Area of Advance at Chalmers. These supports are gratefully acknowledged.

REFERENCES

Benilov, M.S. and A. Marotta, A (1995). A model of the cathode region of atmospheric pressure arcs. *Journal of Physics D: Applied Physics*, **28**, pp. 1869-1878.

Benilov, M.S. (2008). Understanding and modelling plasma–electrode interaction in high-pressure arc discharges: a review. *Journal of Physics D: Applied Physics*. **41**, 144001-15.

Cayla, F. (2008). *Modélisation de l'interaction entre un arc électrique et une cathode*. PhD. Thesis, Université Toulouse III-Paul Sabatier, France.

Choquet, I. and B. Lucquin-Desreux (2005). Hydrodynamic limit for an arc discharge at atmospheric pressure. *Journal of statistical physics*. **119**, pp. 197-239.

Choquet, I. and B. Lucquin-Desreux (2011). Non equilibrium ionization in magnetized two-temperature thermal plasma. *Kinetic and Related Models*. **4**, pp. 669-700.

Choquet, I., A. Javidi and H. Nilsson (2012). On the choice of electromagnetic model for short high-intensity arcs, applied to welding. *Journal of Physics D: Applied Physics*. **45**, 205203.

Luhmann, J., S. Lichtenberg, O. Langenscheidt and M.S. Benilov (2002). Determination of HID electrode falls in a model lamp I: pyrometric measurements. *Journal of Physics D: Applied Physics*. **35**, 1631-1638.

Füssel U., M. Lohse, and S. Rose (2014). Sheath modelling for TIG welding. IIW Commission IV-XII-SG212, Intermediate Meeting, Wels, Austria.

Hsu, K.C., K. Etemadi, and E. Pfender (1983). Study of the free-burning high-intensity argon arc. *Journal of Applied Physics*. **54**, pp. 1293-1301.

Javidi Shirvan, A. (2013). *Modelling of electric arc welding: arc-electrode coupling*. Lic. Thesis, Chalmers University of Technology, Sweden.

Lowke, J. J. and M. Tanaka (2006). LTE-diffusion approximation for arc calculations. *Journal of Physics D: Applied Physics*. **39**, pp. 3634-3643.

Sansonnens, L., J. Haidar and J.J. Lowke (2000). Prediction of properties of free burning arcs including effects of ambipolar diffusion. *Journal of Physics D: Applied Physics*. **33**, pp. 148-157.

Sass-Tisovskaya, M. (2009). *Plasma arc welding simulation with OpenFOAM*. Lic. thesis, Chalmers University of Technology, Sweden.

Vacquié, S. (2000). *L'arc électrique*. CNRS Editions, Eyrolles Paris.

Zhou, X. and J. Heberlein (1999). Analysis of the arc-cathode interaction of free-burning arcs. *Plasma Sources Science and Technology*. **3**, pp. 564-568.